JOURNAL OF GEOPHYSICAL RESEARCH, VOL. 105, NO. D6, PAGES 7177–7186, MARCH 27, 2000

Some observational and modeling evidence of long-range transport of air pollutants from Europe toward the Israeli coast

Aryeh Wanger,[1] Mordechai Peleg,[1] Geula Sharf,[1], Yitzhak Mahrer,[2] Uri Dayan,[3] George Kallos,[4] Vassiliki Kotroni,[4] Konstantinos Lagouvardos,[4] Maria Varinou,[4] Anastasios Papadopoulos[4] and Menachem Luria[1]

Abstract. The present paper reports results of a study that attempted to elucidate the factors causing relatively high levels of particulate sulfate that have frequently been observed over central Israel. Aircraft research flights were performed some 70 km west of and parallel to the Israeli coastline during September 1993 and June 1994. Comparison between the two measurement periods revealed a distinctive difference between the two different sampled air masses. While both air masses were nearly homogeneous throughout the measurement period and along the180 km flight path, the air mass sampled in September 1993 was much "cleaner" than the air mass sampled during June 1994. The concentrations of the air pollutants measured during the 1993 campaign averaged 0.7 ± 0.4 parts per billion by volume (ppbv) SO_2, 1.0 ± 0.6 ppbv NO_y, 39 ± 7 ppbv O_3 and 38 ± 7 nmol/m^3 particulate sulfate, whereas in the second period the levels averaged 3.0 ± 1.0, 3.9 ± 1.8, 48 ± 9, and 108 ± 63, respectively. These results suggest that the two air masses traveled different paths before reaching the eastern Mediterranean region. Further examination of the air mass sources and transport were performed using the Regional Atmospheric Modeling System for meteorological simulations and the Hybrid Particle and Concentration Transport Package for dispersion modeling. The model simulation showed that during the 1993 measurement period, the pollution sources in southern Europe and the Balkans did not effect the eastern coasts of the Mediterranean, while the synoptic conditions and simulation results for the June 1994 period indicated that the winds over the eastern Mediterranean tended to be northwesterly and thus forcing the polluted air masses toward the coast of Israel.

1. Introduction

The synoptic conditions prevailing in the eastern Mediterranean (EM) area during the summer months, June through September, are fairly consistent. In the east, the monsoonal trough leads to the development of a thermal low-pressure trough over southern Asia that extends westward over the northeastern Mediterranean region. This system is known as the "Persian Trough." To the west, the expanded Azores anticyclone dominates the western part of the region. The anticyclone character of the large-scale circulation aloft causes subsidence, restricting the boundary layer formed by the Persian Trough to about 300m in depth. The prevailing winds in the EM are generally northwesterly reinforced by the sea breeze. However, the flow patterns over the region are more complicated, mainly because of topographic and thermal effects. The presence of islands and peninsulas in the sea, as well as mountain barriers and the gaps between them, acts as channels for air masses in the areas surrounding the sea. Further, the temperature gradient between the land masses of southern Europe and the Mediterranean waters and between the Mediterranean waters and the hot arid land of North Africa also affects the wind flows [*Kallos* et al., 1996, 1998].

Climatological studies of back trajectories in the region have shown that during about 70% of the year, air masses arriving at the Israeli coast originate in either southwestern or in southeastern Europe. This effect is even more pronounced during the summer months [*Dayan*, 1986]. Thus polluted air parcels can be transported thousands of kilometers within the stable marine boundary layer of the Mediterranean without significant dilution [*Kallos et al.*, 1993]. During transportation, the intensive solar radiation existing during the summer months enhances photochemical reactions in those parcels, while the prevalent dry conditions limit deposition removal processes.

Long-range transport of air pollutants has already been shown to affect the air quality of remote sites at various regions in the world. *Sasaki et al.* [1988] found that the concentrations of secondary pollutants such as NO_3^- and SO_4^{2-} increase significantly during the transport of air masses from Tokyo Bay to the mountain regions in central Japan, some several hundred kilometers. *Hastie et al.* [1988] also showed that polluted air masses leaving the eastern coast of the United States impacted Bermuda within several tens of hours after having traveled some 1000 km over the Atlantic Ocean. During this transport time, the concentration levels of SO_2 diminished by a factor of 20, whereas the particulate sulfate concentration remained the same. This relatively rapid depletion of S over the Atlantic Ocean suggests fairly efficient processes for transformation of SO_2 to SO_4^{2-} and depletion of SO_2 and SO_4^{2-} by dry deposition.

[1]Environmental Sciences Division, School of Applied Science, The Hebrew University of Jerusalem, Jerusalem, Israel.

[2] Faculty of Agriculture, Food, and Environmental Quality Sciences, The Hebrew University of Jerusalem, Rehovot, Israel.

[3]Department of Geography, The Hebrew University of Jerusalem, Jerusalem, Israel.

[4]Department of Applied Physics, Meteorology Laboratory, National and Kapodistrian University of Athens, Athens, Greece.

Paper number 1999JD901060.
0148-0227/00/1999JD9001060$09.00

Air quality studies performed in Israel have shown that recirculation phenomena can give rise to elevated pollution levels at coastal sites. *Robinson et al.* [1992] used a mesoscale meteorological model to explain an elevated SO_2 episode that occurred in Ashdod (a city approximately 20 km south of Tel Aviv in the coastal plain of Israel). They showed that SO_2 emitted at night from a power plant and the oil refineries was transported by the land breeze off coast into the Mediterranean before being recirculated inland the following day under the influence of the sea breeze. *Alper-Siman Tov et al.* [1997] measured the effects of recirculation patterns at a site on the northern Israeli coast. In this case, air masses that contained elevated levels of nitrogen oxides and hydrocarbons during their off-coast transportation were recirculated inland, under conditions of photochemical activity in daylight, giving rise to elevated ozone levels in addition to elevated nitrogen oxides levels. Similarly, episodes of high O_3 concentration have been reported at sites some 50 km downwind from the metropolitan area of Tel Aviv, several hours after morning rush hour emissions of primary pollutants [*Peleg et al.*, 1994].

Luria et al. [1996] showed in an extensive 10-year experimental study that sulfate levels in Israel have a typical yearly mean of 100 ± 15 nmol/m^3, peaking during the summer to levels up to 500 nmol/m^3. These observed elevated levels can not be explained by local SO_2 emissions sources, estimated by the *Israeli Ministry of the Environment* [1995] as 0.12 Tg S yr^{-1}. Additionally, the sulfur airmass age (SAA, i.e., ratio of sulfate to total S) is usually greater than 0.5, suggesting an aged air mass originating from a remote source. Further, a recent study performed at a coastal site in Israel has shown that incoming air masses have ozone levels of 30-60 parts per billion (ppbv), while primary pollutant (SO_2 and NO) levels in the same air masses were usually at background levels of less than 0.5 ppbv [*Alper-Siman Tov at el.*, 1997].

To investigate further the contribution of long-range transport to air pollution levels monitored at the Israeli coast, a comprehensive study that included 150 hours of instrumented aircraft monitoring flights was performed between 1993 and 1995. The present paper discusses two events of air mass transport that were observed during the research periods and may represent two different types of long-range transport and compare the observed results to model simulation studies.

2. Experiment

The aircraft used in the present investigation was a twin-engine Cessna 310. The instrument package installed in the aircraft included a high-sensitivity SO_2 analyzer (TEII 43S, pulsed fluorescence method, ±0.1 ppbv sensitivity), a high-sensitivity NO-NO_y analyzer (TEII 42S, chemiluminescence method, ±0.1 ppbv sensitivity), and an ozone monitor (Dasibi 1008 AH, UV photometric method, ±2 ppbv sensitivity), as well as a semiautomatic sulfate aerosol sampler and temperature, relative humidity, and pressure-altitude sensors. The zero levels of the monitors were verified both on the ground and in the air, using a PbO scrubber for SO_2, purafil/activated charcoal for NO_y, and activated charcoal for ozone. Span calibrations were performed daily on the ground before takeoff. The aerosol sampler consisted of a five-filter holder system fitted outside the aircraft so that the air sampled came directly in contact with the filters without interference of contaminating materials. During each flight a dynamic blank was taken in addition to the actual aerosol samples taken during the different flight legs. The sampling flow rates were continuously measured and recorded using a massflow meter. Filters for particulate sulfate collection (Millipore Falp 047, 1-μm pore size, Teflon filters) were prewashed in Na_2CO_3 solution and in triple-distilled water, before being vacuumed dried [*Parrish et al.*, 1993]. After aerosol extraction from the filters, sulfate analysis was performed using an ion chromatographic technique [*Baltensperger and Hertz*, 1985]. A global positioning system (GPS) was used to continuously monitor the position of the aircraft during the research flight. The data were recorded every 10 s and stored on both on a personal computer and a data logger.

The flight paths taken were approximately 70 km offshore, parallel to the Israeli coastline, and 180 km in length with Tel Aviv in the center (Figure 1). Two separate measuring legs were performed during each research flight, one round trip from the starting point toward the north and the second toward the south (flight paths 1 and 2, respectively). All flights were performed during midday under westerly wind flow conditions and at altitudes of about 300 m (well within the boundary mixing layer). The first series of measurements was performed between September 5 and 9, 1993, and the second was performed between June 15 and 21, 1994.

Data for the synoptic analysis for the model simulation were from the European Center for Medium Weather Forecast (ECMWF).

3. Model Description

The regional-scale transport mechanism was investigated by using the Regional Atmospheric Modeling System (RAMS) and

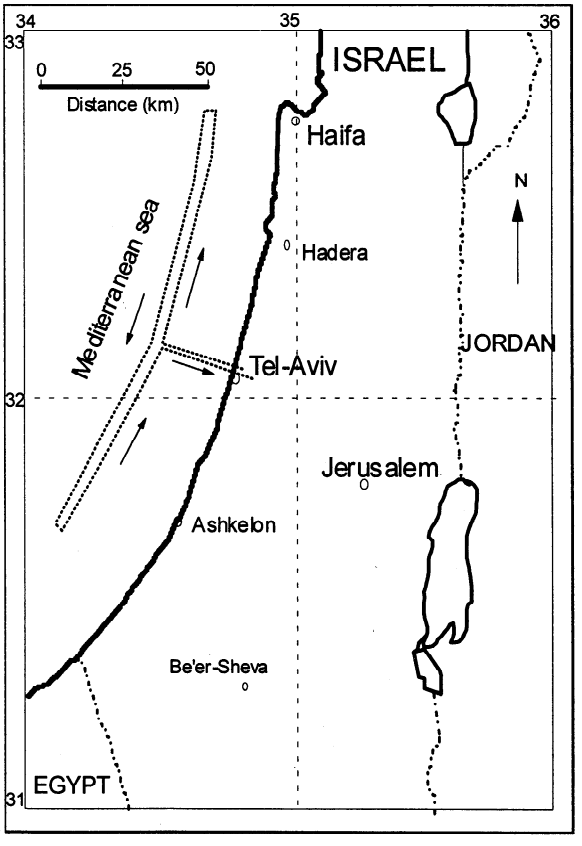

Figure 1. Air sampling flight paths (dotted lines) off the coast of Israel.

the Hybrid Particle and Concentration Transport Package (HYPACT) model.

The RAMS is a highly versatile numerical code developed at Colorado State University for simulating and forecasting meteorological phenomena (*Pielke et al.*, 1992). The model is constructed around the full set of primitive dynamical equations which govern atmospheric motions and supplements these equations with optional parameterizations for turbulent diffusion, solar and terrestrial radiation, moist processes including the formation and interaction of clouds and precipitating liquid and ice, sensible and latent heat exchange between the atmosphere, multiple soil layers, a vegetation canopy, surface water, the kinematics effects of terrain, and cumulus convection. Two-way interactive grid nesting in RAMS allows local fine mesh grids to resolve compact atmospheric systems such as thunderstorms, while simultaneously modeling the large-scale environment of the systems on a coarser grid.

RAMS has four different options for moisture calculations. In the present study, flag NLEVEL=2 was used, which activates condensation of water vapor to cloud water whenever supersaturation is attained. According to this, the partitioning of the total water substance into vapor and cloud water is always purely diagnostic. No other forms of liquid or ice water were considered. Both the positive buoyancy effect of water vapor and the liquid water loading of cloud water are included in the vertical equation of motion. Radiative effects of both water vapor and cloud water are activated, if the radiation parameterization is itself activated. The simulated cases were those with weather conditions in favor of long-range transport. The above level of microphysical complexity was considered adequate to cover the variety of phenomena observed during these periods with a reasonable usage of computer resources.

For the dispersion calculations, the HYPACT model was used. This model is a combination of a Lagrangian particle model and a Eulerian concentration transport model (*Tremback et al.*, 1994). It utilizes the velocity and turbulence fields simulated by RAMS. Almost any type of sources can be specified anywhere in the domain, and the emissions can be instantaneous, intermittent, or continuous.

4. Results and Discussion

Air pollutant concentrations for the six parameters monitored during the two flight campaigns, September 1993 and June 1994, are presented in Table 1. Comparison of the two measurement periods reveals a distinct difference between the two air masses examined. While both air masses are nearly homogenic throughout the measurement period and all along the flight paths, the air mass sampled during September 1993 is much "cleaner" than the air mass sampled in June 1994. Air pollutant concentrations averaged for the first period 0.7 ± 0.4 ppbv SO_2, 1.0 ± 0.6 ppbv NO_y, 39 ± 7 ppbv O_3, and 38 ± 7 nmol/m^3 particulate sulfate as compared to3.0 ± 1.0, 3.9 ± 1.8, 48 ± 9, and 108 ± 63, respectively, for the second period. As is shown in Figure 2, the June

Table 1. Flight Air Pollution Measurement Results for September 1993 and June 1994 off the Israeli Coast

Date	Time[a]	Path	Particulate Sulfate nmol/m^3	SO_2 ppbv	No_y ppbv	NO ppbv	NO_y-NO ppbv	O_3 ppbv
Sep. 5, 1993	1400	1, 2[b]	---	1.3 ± 0.1	1.8 ± 1.9	1.3 ± 2.6	0.5 ± 2.6	48 ± 1
		1, 2	43					
Sep. 6, 1993	1400	1, 2	49	1.0 ± 0.1	Nd	0.4 ± 0.1	Nd	38 ± 1
		1, 2	46					
Sep. 7, 1993	1400	1, 2	40	0.5 ± 0.1	1.0 ± 0.3	0.2 ± 0.1	0.8 ± 0.3	28 ± 1
		1, 2	41					
Sep. 8, 1993	1300	1, 2	19	0.2 ± 0.1	0.7 ± 0.2	0.2 ± 0.1	0.5 ± 0.2	41 ± 1
		1, 2	30					
Sep. 9, 1993	1300	1, 2	46	0.4 ± 0.1	0.5 ± 0.3	0.5 ± 0.1	0.0 ± 0.3	39 ± 1
		1, 2	32					
Jun. 15, 1994	1630	1	81	2.7 ± 0.3	3.1 ± 3.2	1.1 ± 0.5	2.0 ± 0.4	42 ± 8
	1715	2	124	2.5 ± 0.4	2.5 ± 0.2	0.9 ± 0.4	1.5 ± 0.5	46 ± 7
Jun. 16, 1994	1250	1	158	1.5 ± 0.1	4.4 ± 0.6	0.8 ± 0.3	3.6 ± 0.6	43 ± 3
	1320	2	61	1.4 ± 0.1	3.7 ± 0.5	0.6 ± 0.3	3.1 ± 0.6	42 ± 3
	1650	1	nd	4.5 ± 0.1	3.3 ± 0.5	1.1 ± 0.4	2.2 ± 0.3	42 ± 3
	1720	2	250	4.3 ± 0.1	3.2 ± 0.4	1.1 ± 0.5	2.1 ± 0.4	42 ± 4
Jun. 19, 1994	1300	1	18	2.9 ± 0.2	5.7 ± 0.3	0.7 ± 0.1	5.0 ± 0.3	43 ± 4
	1745	2	119	2.4 ± 0.2	6.3 ± 0.3	0.8 ± 0.1	5.5 ± 0.3	42 ± 4
Jun. 20, 1994	1250	1	97	3.8 ± 0.3	1.7 ± 0.2	1.1 ± 0.1	0.6 ± 0.2	61 ± 7
	1330	2	75	3.1 ± 0.2	2.0 ± 0.3	1.1 ± 0.1	0.8 ± 0.3	65 ± 6
Jun. 21, 1994	1220	1	92	3.7 ± 0.4	7.3 ± 0.4	1.5 ± 0.1	5.8 ± 0.4	60 ± 5

Here nd means not detected

[a]Time is for the middle of the flight leg.

[b]During the 1993 flights, only one filter sample was taken for both path 1 and path 2.

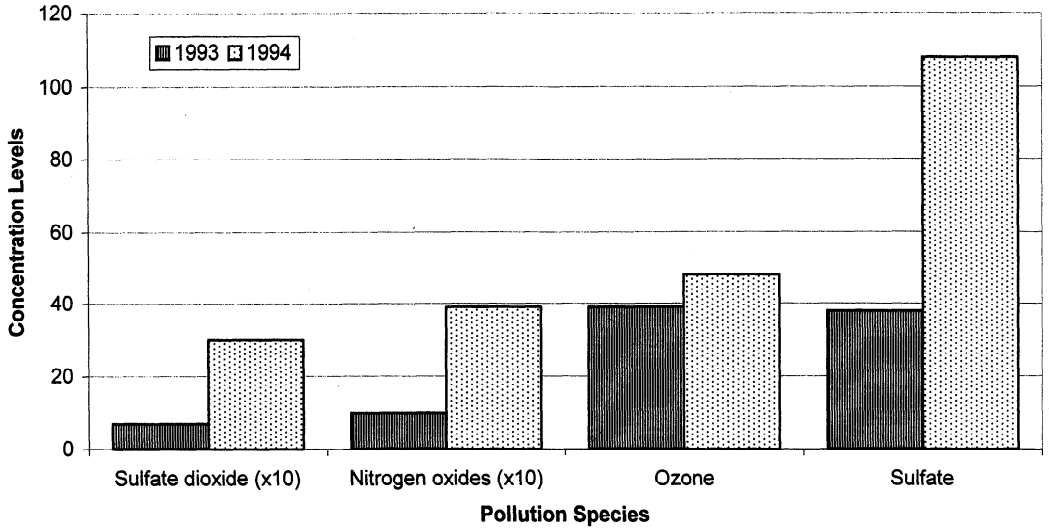

Figure 2. Flight air pollution measurement results for September 1993 and June 1994 off the Israeli coast.

1994 averaged concentrations showed almost a fourfold increase for the primary pollutants, threefold increase for the sulfates, and only a 20% increase for ozone, as compared to September 1993. The above results imply that the air masses followed different paths before reaching Israel.

5. Model Simulation Studies

Model simulations using the two previously mentioned models were performed in order to understand the reasons for the differences in the pollution content of the long-range transported air masses that arrived at the eastern part of the Mediterranean Sea.

5.1. September 1993 Episode

5.1.1. Synoptic conditions. At the beginning of the period (September 4), a barometric trough extended from northern Europe to Italy at the 500-hPa level. A cold surface low was formed over the Balkans, under its area of upperlevel divergence. In the eastern Mediterranean, at the 500-hPa level, north westerly flow prevailed accompanied at the surface by a local high (Figures 3a-3b). From September 5 through the end of the event, the anticyclonic subsiding conditions evolved at shallow to middle tropospheric layers over the eastern Mediterranean as a result of a surface high-pressure system accompanied by an upperair ridge. Concurrently, over the Balkan region, a weak wavecyclone is observed with baroclinic instability contained in the shallow atmospheric layers. This weak perturbation did not initiate a significant temperature advection. The frontal zone was very weak and was associated with relatively weak convective activity over NW Greece in the afternoon hours of September (Figures 3a-3c). In general, barotropic conditions were prevailing in most of the Eastern Mediterranean region during this period.

5.1.2. RAMS model simulation. The simulation was performed for 10 days (September 1-10, 1993). A resolution of 1.0 deg latitude/longitude of ECMWF analysis fields was used for the RAMS model initialization. The grid selected covering an area of 6000 × 3000 km^2 (from the Atlantic Ocean at 15°W to the Caspian Sea at 50°E and from the Sahara Desert at 25°N to central Europe at 50°N) with a horizontal increment of 60 km. During the first 3 days, westerly flows were observed over the central Mediterranean. Light northeastern flow prevailed over the Aegean Sea, and local thermal circulation developed during the day, forming a convergence zone over the Greek peninsula. The flow backed to a northwestern direction at the exit of the Aegean Sea and the eastern Mediterranean. This flow pattern was consistent with the surface synoptic configuration observed for that day. The flow weakened on September 4 and meandered with no distinct direction on its way from the Aegean Sea toward the eastern Mediterranean. On September 5 at 1200 UTC (Figure 4) a southwesterly flow was evident in the central Mediterranean and Greek peninsula, in good agreement with the synoptic situation (approach of the frontal system). This southwesterly flow was also reported by the surface stations located along the western coast of Greece and over the islands in the central and northern Aegean Sea. The discontinuity associated with the frontal system was evident in the near-surface wind pattern over the straits between Italy and Greece. Weak western flows prevailed over the eastern Mediterranean during the same period. On September 6, the system moved away over Turkey, and the flow over the Aegean Sea veered to a northwesterly direction and later to a northerly one. Over the eastern Mediterranean the flow was still westerly and somewhat stronger (1-2 m/s) than the previous day's flow. Two days later, on September 7 and for the rest of the simulation period, the wind flow pattern was northeasterly over the north Aegean Sea and westerly over the eastern Mediterranean. Local thermal circulation developed during the day and weakened during the night, according to the prevailing synoptic conditions with the establishment of a high pressure over the Balkans and a weak pressure gradient over the area.

5.1.3 Dispersion simulations. When a relatively large cyclonic system is located over Europe, the synoptic flow is generally from the west in the western and central Mediterranean. This system moves the polluted air masses located over the western or central part of the Mediterranean toward the eastern Mediterranean. Major urban areas along the Mediterranean coasts were therefore specified as emission sources for the HYPACT simulation that started on September 5 1993, at 0000 UTC and lasted 96 hours. The city sources chosen were Barcelona (Spain), Lyons (France), Rome and Trieste (Italy), Messina (Sicily, Italy), Athens and Thessaloniki (Greece), Constanza

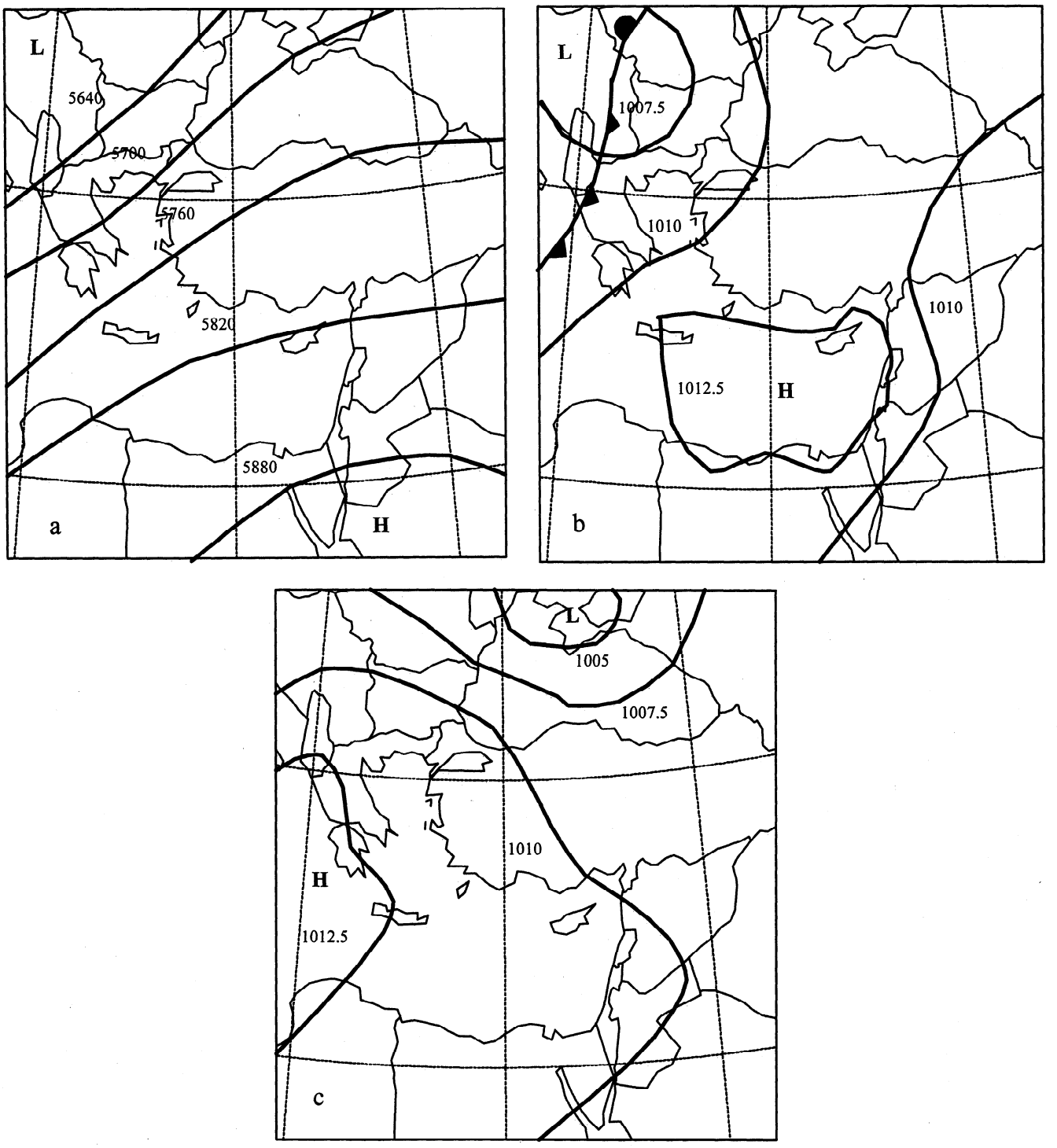

Figure 3. Synoptic analysis for case 1 in September 1993. (a) Geopotential height (in meters) at 500 hPa, September5 at 0000 UTC. (b) Surface synopotic situation, isobar values given in hectopascals, September 5 at 1200 UTC. (c) Surface synopotic situation, isobar values given in hectopascals, September 6 at 1200 UTC.

(Romania), and Istanbul (Turkey). At 0600 UTC on September 6 1993, after 30 hours of particle release, the plume from Sicily was transported by the westerly flow toward the Aegean Sea. The more recently released particles were confined within a narrow zone indicating weak dispersion conditions in the stable marine boundary layer.

The particles released from Athens and Thessaloniki were transported northeasterly over the Bosporus and Dardanelles in the Black Sea area and were dispersed more widely owing to the thermal and topographic effects during transport over the land areas. Figure 5 presents the position of the particles at 1500 UTC on September 6 1993, 39 hours after particle release. The plume from Sicily is transported over the Aegean Sea through the gap between the Greek mainland and the Island of Crete. Over the Aegean Sea, after the passage of the synoptic system, the prevailing wind had a northwesterly direction. The newly re-

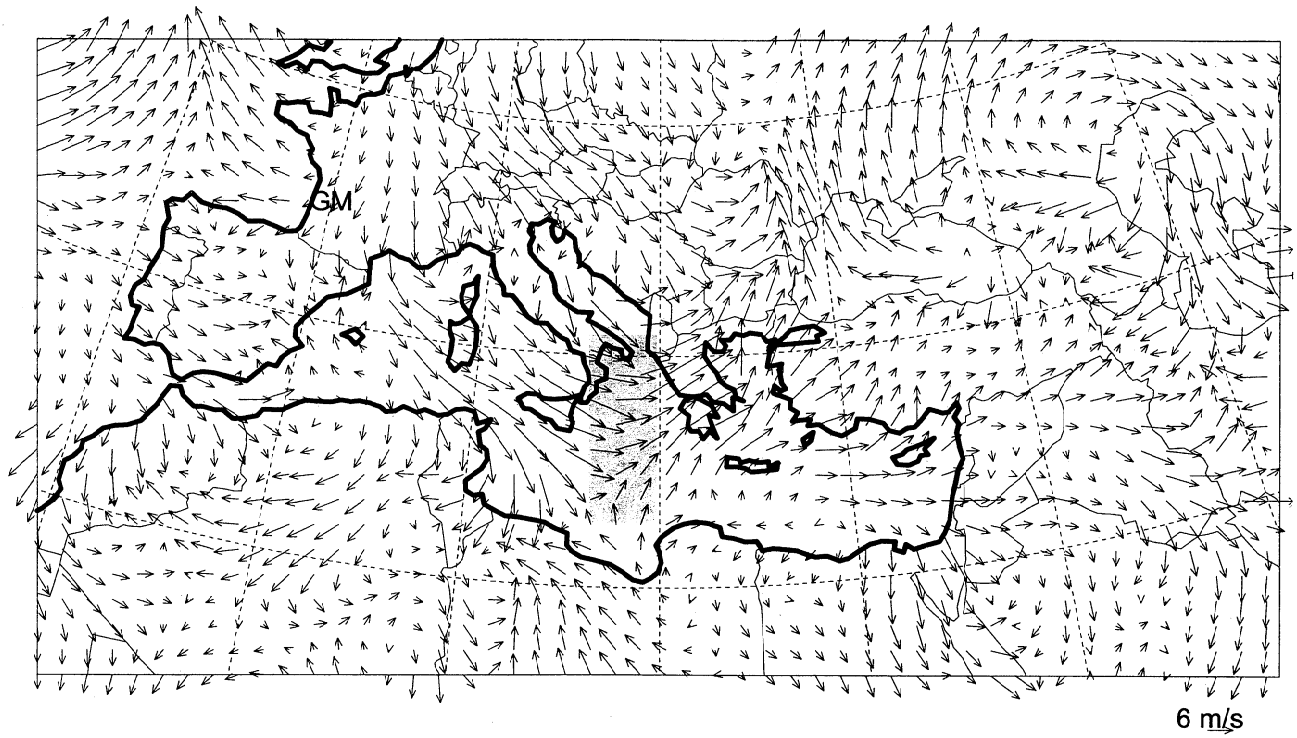

Figure 4. Wind field model simulation for September 5, 1993, at 1200 UTC, altitude 39 m. Wind arrows are plotted every 120 km.

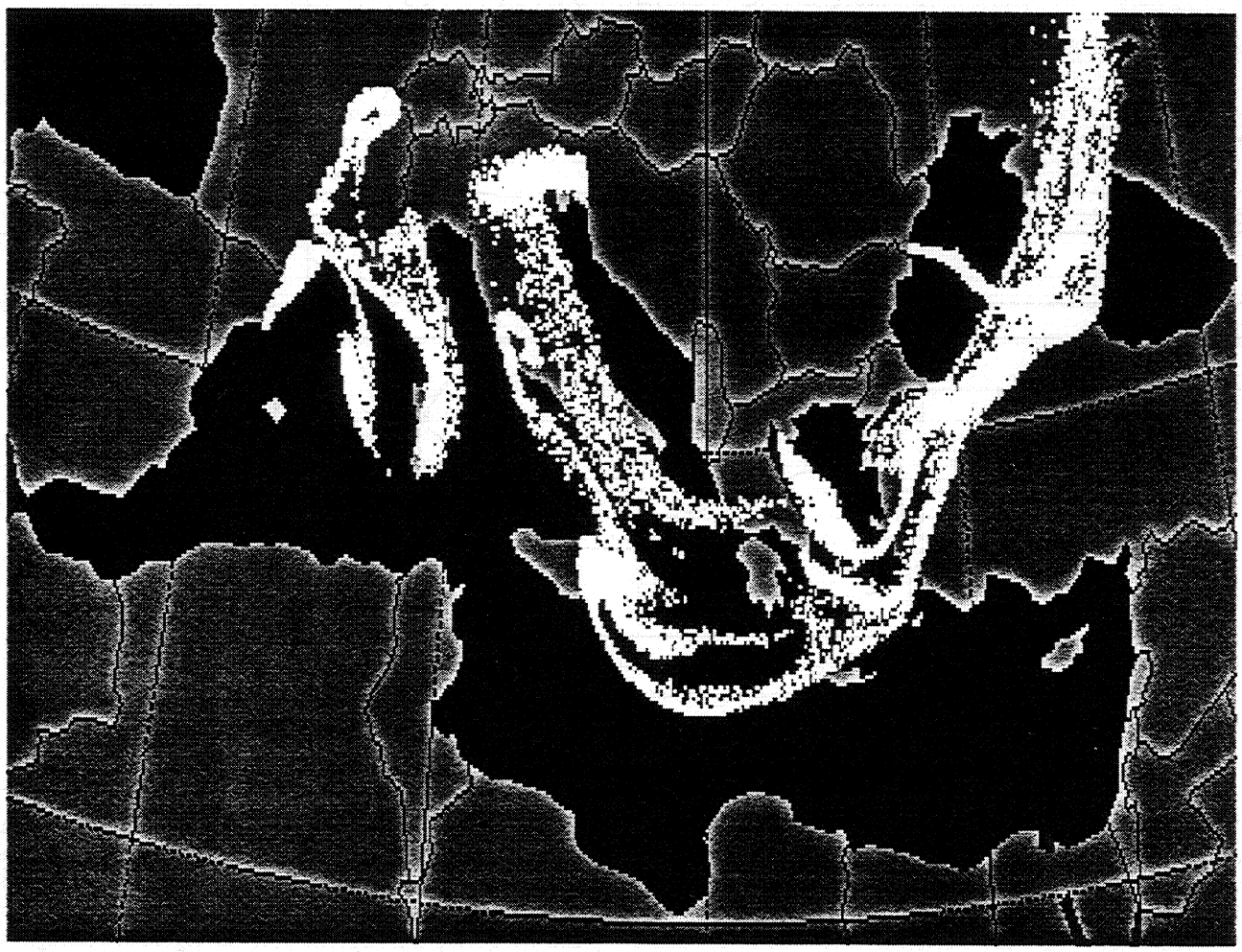

Figure 5. Particle positions for September 6, 1993, at 1500 UTC (ground level, 39 hours after particle release) as calculated by the HYPACT dispersion model. The continuously released sources were from Barcelona (Spain), Lyons (France), Rome and Trieste (Italy), Messina (Sicily, Italy), Athens and Thessalonoki (Greece), Constanza (Romania), and Istanbul (Turkey).

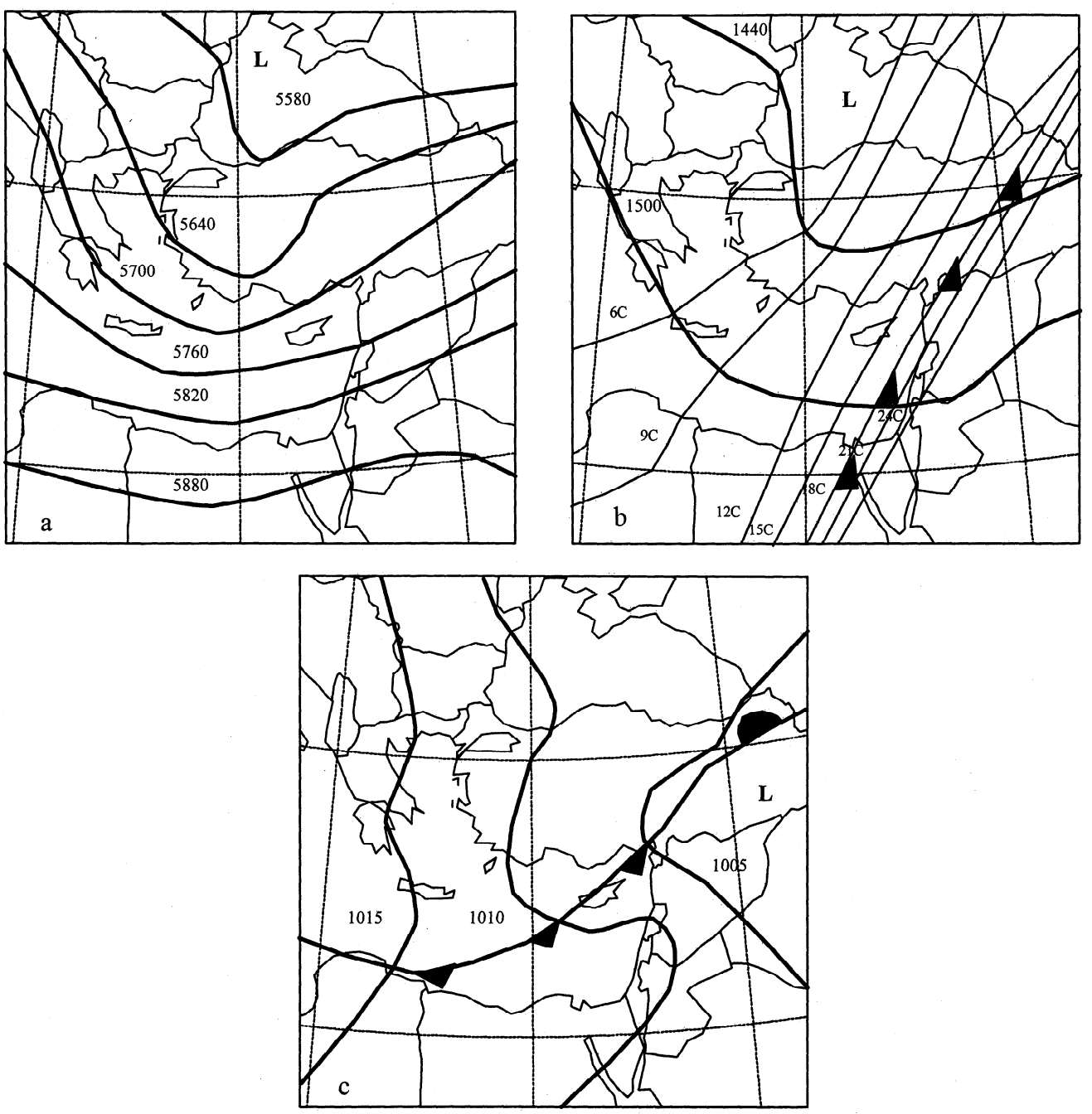

Figure 6. Synoptic analysis for case 2, on June 16, 1994. (a) Geopotential height (in meters) at 500 hPa, June 16, at 0000 UTC. (b): Geopotential height (in meters) for 850 hPa, June 16, at 0000 UTC, isotherms in degrees Centigrade. (c) Surface synopotic situation; isobar values given in hectopascals, 16 June at 0600 UTC.

leased particles from Athens and Thessaloniki were transported southeasterly over the southern and eastern Aegean Sea while the old plumes were transported northeasterly over Turkey. Under these conditions, it is obvious that the plume pathways arriving from southern Europe and the Balkans were not directed toward the eastern coasts of the Mediterranean. Air masses approaching the Israeli coasts from the west during the experimental measurement period had a relatively long history over the sea. It is also possible that these air masses were previously transported, a few days earlier, to the Mediterranean from polluted areas in Europe (before the simulation period). But, in this case, these air masses were "cleaned up" over the Mediterranean waters. Either way, the pollutant concentrations in these air masses reaching Israel are expected to be low, in agreement with the experimental results of that period.

5.2. June 1994 Episode

5.2.1. Synoptic conditions. For June 16 1994, a shallow cyclone formed over the northeastern Mediterranean region caused a gradual deepening of the Persian Trough accompanied by a weak cold front that swept the EM basin (Figure 6a-6b). While these conditions led to a rather cool spell over the EM as manifested by a deepening of the marine turbulent boundary layer,

converging air aloft was observed over the Balkans region. This convergence enhanced a rise of surface air pressure, suppressing any precipitation convective element. This front acted as a converging zone during its movement eastward and crossed the Israeli coasts toward noon. Barotropic conditions prevailed during the entire period over the whole EM region.

This analysis emphasizes the importance of air mass convergence for the built-up mechanism of an advancing pollutant front steered by the atmospheric flow aloft. During a period of 6 days, three waves of air masses with elevated air pollution concentrations originating in southeastern Europe reached the Israeli coasts and confirmed the higher levels of air pollutants measured during that time. Although the increase in the primary pollutant levels is about 4 times that of the first episode, the absolute levels of the secondary pollutants in the latter case are more significant. These results are of particular importance with respect to sulfate particulate, which increased by a factor of 3, since they are known to adversely affect human health [*Dockery et al.*, 1993].

5.2.2. RAMS model simulation. The simulation was performed for 5½ days, beginning June 14 1994, at 0000 UTC. A resolution of 0.5 deg latitude/longitude of ECMWF analysis fields was used for the RAMS model initialization. In order to observe in more detail the air mass transport toward the eastern Mediterranean, the horizontal grid increment had to be reduced to 20 km, and as a result the simulation domain had to be smaller as well. The domain covered an area of 2800 × 2600 km^2 between longitudes of 20° and 50°E and between latitudes 22° and 48°N. A second grid was nested inside the coarser grid to resolve local phenomena. This grid covered most of Israel and the Israeli coasts. It included an area of 200 × 180 km^2, centered at 32°30′E, 35°N and 28 vertical levels that reached an altitude of 14,500 m using a σ coordinate system.

The simulation results were in good agreement with the synoptic analysis. The model wind field analysis revealed that on June 14 at 1200 UTC, northeasterly winds prevailed in the Aegean Sea and northwesterly winds were in the junction area of the Aegean Sea and the Mediterranean. At the same time, northwest wind flows existed off the Israel and North Africa coasts. On June 15 at 1200, the winds were northwesterly in the Aegean Sea, north northwesterly in North Africa and westerly off the coasts of Israel. On June 16 and 17, flows from Greece toward Israel were direct and rapid. The wind field diagram for June 17 at 1200 UTC (Figure 7) shows that the winds in this region were westerly after the passage of the convergence zone. During the rest of the simulation period the winds over the eastern Mediterranean were from a northwesterly direction, thus forcing air mass migration toward the south of Israel.

5.2.3. Dispersion simulations. Based on the meteorological fields generated by RAMS a few particle release scenarios were performed for the test case. Particles were released from one or two sources at a time, beginning on June 14 at 0000 UTC, and continued for 100 hours. The particle release layer was between the ground and up to an altitude of 100 m above sea level. In one simulation, the particles were released from Athens, Greece on June 14 at 0000 UTC. At the start, the movement of the plume in the Aegean Sea was cyclonic, and the plume traveled toward western Turkey. After 48 hours the older particles were widely dispersed over Turkey because of the topographic and thermal effects over the land. The newly released particles, in contrast, were transported in a narrow front through the straits between the Greek islands of Crete and Rhodes, south of Cyprus, and toward Alexandreta Bay (Turkey) along with strong southerly winds that prevailed west of the coast of Israel. Figure 8 shows the dispersion of the particles on June 16 at 0000 UTC.

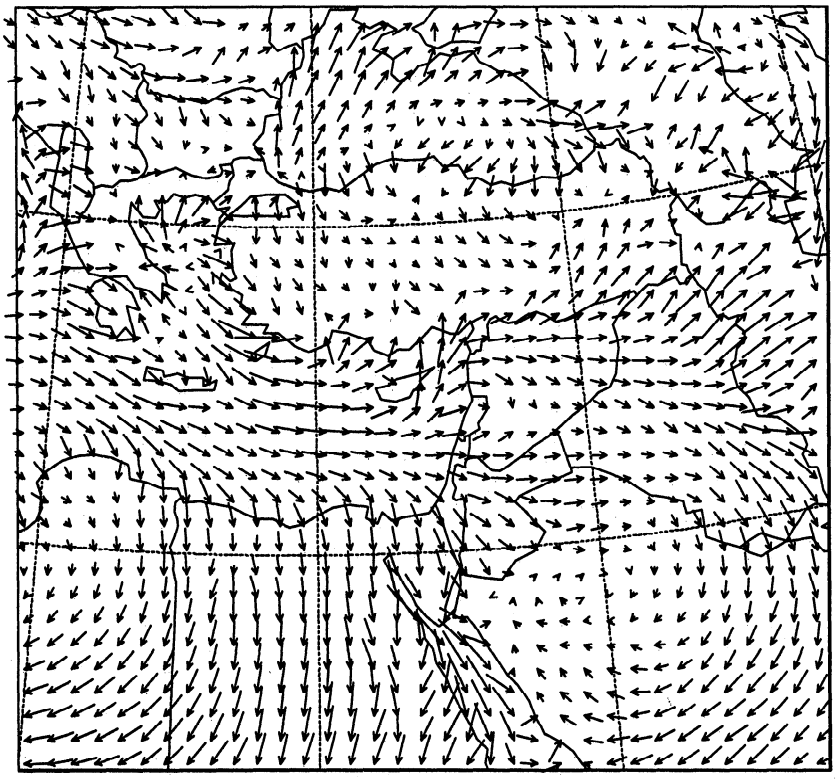

Figure 7. Wind field model simulation for 1200 UTC on June 17, 1994, at an altitude of 78 m. Wind arrows are plotted every 40 km. Vector scale, each mm equivalent to 2.5 m/s.

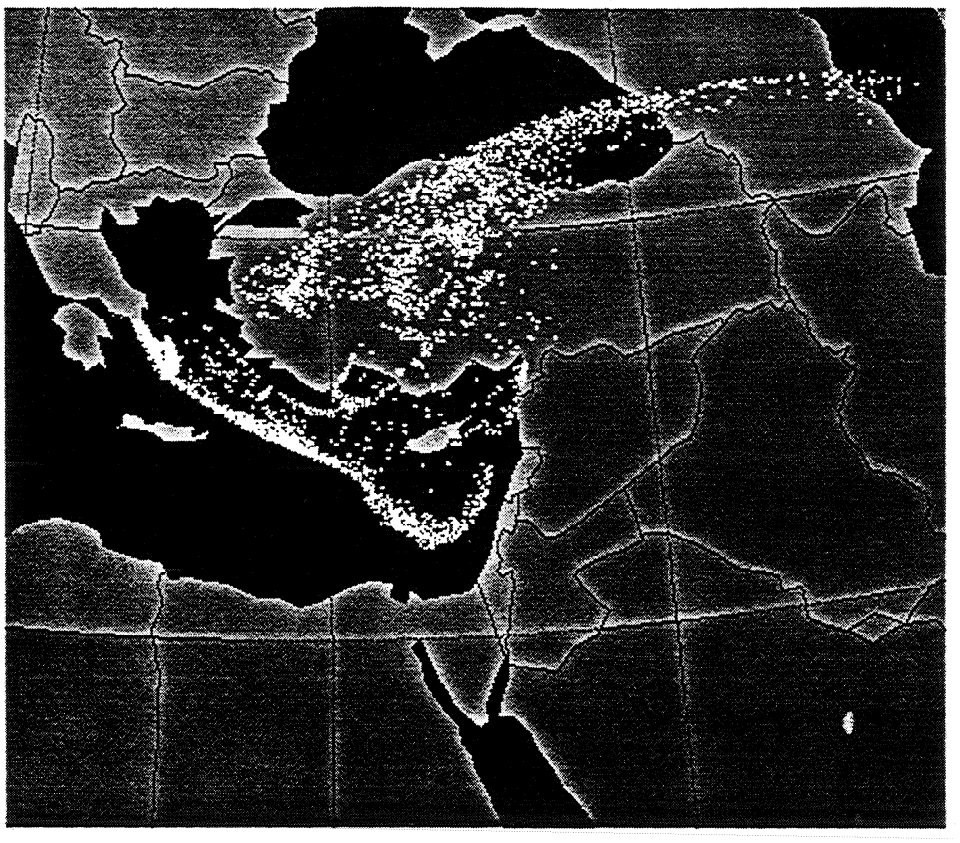

Figure 8. Particle positions as calculated by the HYPACT dispersion model. Particles were released from Athens (Greece) on June 14, 1994, and are shown after dispersion duration of 48 hours.

During that day, after the passage of the converging zone and the veering of the wind to the northwest, the particle cloud penetrates the coast of Israel. A comparable situation was also observed between June 17 and June 18. During this episode, the Athens plume covered the entire eastern Mediterranean region within 60 hours. A similar dispersion pattern was also observed for particles released from other cities such as Izmir (Turkey) or even more remote sources such as Burgas (Bulgaria).

6. Conclusions

The results from the aircraft measurements performed in the present study together with model simulations have shown that the eastern Mediterranean region can be affected by pollutant emission sources thousands of kilometers upwind. While this phenomenon was expected from climatological observations, it has now been confirmed for the first time by aircraft measurements and supported by computer simulations using a dynamic model. Two episodes of long-range transport were selected for intensive study. The synoptic conditions that caused the elevated pollution levels at the Israeli coast during the June 1994 episode and the "clean" background pollution values observed during September 1993 were characterized using a regional meteorological and dispersion model. The simulation study confirmed the actual airborne measurements performed west of the Israeli coast.

Acknowledgments. This research was funded by the DG-XII of the European Union through research contract AVI-CT92-005 (T-TRAPEM). The authors would like to thank Ilan Seter of the Israeli Meteorological Service for valuable discussions and information concerning the synoptic conditions existing in the region during the experimental periods.

References

Alper-Siman Tov, D., M. Peleg, V. Matveev, Y. Mahrer, I. Seter, and M. Luria, Recirculation of polluted air masses over the east Mediterranean coast, *Atmos. Environ., 31* (10), 1441-1448, 1997.

Baltensperger, U., and J. Hertz, Determination of anions and cations in atmospheric acrosols by single column ion chromatography, *J. Chromatog, 324*, 153-161, 1985.

Dayan, U., Climatology of back trajectories from Israel based on synoptic analysis, *J. Clim. Appl. Met. Eorol., 25*, 591-595, 1986.

Dockery, D. W., C. A. Pope, X. Xu., J. D. Spengler, J.D., J. H. Ware, M. E. Fay, B. G. Ferris, and Speizer F.E., An association between air pollution and mortality in six U.S. cities, *New Eng. J. Med., 24*(329), 1753-1759, 1993.

Hastie, D. R., H. I. Schiff, D. M. Whelpdale, R. E. Peterson, and W. H. Zoller, Nitrogen and sulfur over the western Atlantic Ocean, *Atmos. Environ., 22*(11), 2381-2391, 1988.

Israeli Ministry of the Environment, Annual report, vol. 19-20, p. 109, Jerusalem, Israel, 1995.

Kallos, G., P. Kassomenos, and R. A. Pielke, Synoptic and mesoscale weather conditions during air pollution episodes in Athens, Greece, *Boundary Layer Meteorol., 62*, 163-184, 1993.

Kallos, G., V. Kotroni, K. Lagouvardos, A. Papadopoulos, M. Varinou, M. Luria, M. Peleg, A. Wanger, G. Sharf, and G. Tuncel, Transport and transformation phenomena in the eastern Mediterranean, in *Preservation of Our World in the Wake of Change, Proceedings of the Sixth International Conference of the Israeli Society for Ecology and Environmental Quality Sciences*, edited by Y. Steinberger, pp.17, ISEEQS Publ., Jerusalem, Israel, 1996.

Kallos G., V. Kotroni, K. Lagouvardos, and A. Papadopoulos, On the long-range transport of air pollutants from Europe to Africa, *Geophys. Res. Lett.,25*, 619-622, 1998.

Kontroni, V., G. Kallos, and K. Lagouvardos, Convergence zones over the Greek Peninsula and associated thunderstorm activity, *Q. J. R. Meteorol. Soc., 123*, 1961-1984, 1997.

Luria, M., M. Peleg, G. Sharf, D. SimanTov-Alper, N. Spitz, Y. Ben Ami, Z. Gawii, B. Lifschitz, A. Yitzchaki, and I. Seter, Atmospheric

sulfur over the east Mediterranean region, *J. Geophys. Res., 101*(D20), 25,917-25,930, 1996.

Parrish, D .D., et al., The total reactive oxidized nitrogen levels and the partitioning between the individual species at six rural sites in eastern north America, *J. Geophys. Res., 98*(D2), 2927-2939, 1993.

Peleg M., M. Luria, I. Seter, D. Perner, and P. Russell, Ozone levels in central Israel, *Isr. J. Chem., 34*, 375-386, 1994.

Pielke R. A., et al., A comprehensive meteorological modeling system - RAMS, *Meteorol. Atmos. Phys., 49*, 69-91, 1992.

Robinson J., Y. Mahrer, and E. Wakshal, The effect of mesoscale circulation on the dispersion of pollutants (SO_2) in the eastern Mediterranean southern coastal plain of Israel, *Atmos. Environ., 26B*(3), 271-277, 1992.

Sasaki K., H. Kurita, G. R. Carmichael, Y. S. Chang, K. Murano, and H. Ueda, Behavior of sulfate, nitrate and other pollutants in the long-range transport of air pollution, *Atmos. Environ., 27*(7), 1301-1308, 1988.

Tremback, C. J., W. A. Lyons, W. P. Thorson, and R. L. Walko, An emergency response and local weather forecasting software system, in *Proceedings of the 20th NATO/CCMS Technical Meeting on Air* Pollution and Its Application, vol. 10, pp. 423-429, North Atlantic Treaty Organ., Brussels, 1994.

U. Dayan, Department of Geography, The Hebrew University of Jerusalem, Jerusalem 91905, Israel. (e-mail:msudayan@mscc.huji.ac.il)

G. Kallos, V. Kotroni, K. Lagouvardos, A. Papadopoulos, and M. Varinou, Department of Applied Physics, Meteorology Laboratory, National and Kapodistrian University of Athens, Athens 15784, Greece. (e-mail:kallos@skiron.mg.uoa.gr)

M. Luria (corresponding author), M. Peleg, G. Sharf, and A. Wanger, Environmental Sciences Division, School of Applied Science, The Hebrew University of Jerusalem, Jerusalem 91904, Israel. (e-mail:luria@vms.huji.ac.il;pelegm@pob.huji.ac.il)

Y. Mahrer, Faculty of Agriculture, Food, and Environmental Quality Sciences, The Hebrew University of Jerusalem, Rehovot 76100, Israel. (e-mail: mahrer@agri.huji.ac.il)

(Received December 11, 1998; revised September 14, 1999; accepted September 22, 1999)